

Path planning for UAV harvesting information from dynamical wireless sensor nodes at sea

Tu Dac Ho¹, Esten Ingar Grøtli², Tor Arne Johansen³

Abstract—A system of several wireless sensor nodes and one unmanned aerial vehicle (UAV) is considered in this research. The nodes are only floating and drifting with the sea stream. The UAV will be operating as a data mule to gather sensing information from wireless sensor nodes. Unlike prior studies, this paper addressed a realistic ocean model for the nodes movements which will be the references to the Kalman Filter (KF) in estimating for the nodes' positions. Simulation results are evaluated for an optimal flight-able path for the UAV under several constraints by particle swarm optimization (PSO). Specifically, the deviation between the estimated positions and the referenced positions, total energy consumption by the sensors network, data rates between UAV and the nodes, flight time for the UAV, and frequency of visiting the nodes by the UAV will be considered for optimization. The systems performances will be evaluated based on these scenarios: a) an ideal and unrealistic scenario where the UAV follows the nodes continuously; b) a realistic case where the UAV only flies periodically. Discussions and solutions were also addressed for the situations when the deployed nodes are more significantly separated than the cases simulated in the paper.

Keywords: *Data mule, UAV, Kalman Filter, PSO, WSN*

I. INTRODUCTION

An increasing number of applications have used one single unmanned aerial vehicle (UAV) or a swarm of collaborative UAVs in collecting data from wireless sensor networks (WSN). The noticeable benefits of using a UAV compared with a conventional crewed aircraft (e.g., helicopters) are the enhancements in cost, mobility, safety, and the easiness in deployment and operation. In these system applications, UAVs usually play the roles of either a data mule or a data relay node. Some examples of UAVs acting as data mules include ocean monitoring [1], detection and tracking of marine fauna [2], real-time highway surveillance [3], disaster monitoring and management [4],[5], wildfire management and agricultural monitoring [6], and emergency response based on the images taken by UAVs [7]. Examples of UAVs used as relay nodes are for instance, as flyable base stations in the newly rolled 5G network for urban areas [8], as mobile base stations to expand the coverage area of the 5G radio signal to the regions not traversed for emergency services [9], or as mobile relaying node for maritime radio communication system [10]–[12]. The

¹T. D. Ho is with Department of Electrical Engineering, Faculty of Engineering Science and Technology, UiT - The Arctic University of Norway {Tu.D.Ho} at uit.no

²E. I. Grøtli is with Department of Mathematics and Cybernetics, SINTEF Digital, Trondheim, Norway {esteningar.grotli} at sintef.no

³T. A. Johansen is with the Center for Autonomous Marine Operations and Systems (AMOS), Department of Engineering Cybernetics, Norwegian University of Science and Technology, O. S. Bragstads plass 2D, 7491 Trondheim, Norway {tor.arne.johansen} at itk.ntnu.no

UAV can also be used as a flyable base station in relaying mm-Wave radio signal which plays a significant component of the 5G and its beyond cellular networks [13]. In many applications, the prevalent studies to consider include path planning for the UAVs, energy efficiency for data communications, UAV navigation, data links between UAVs and sensor network, energy harvesting, network reliability and throughput, and service availability in such mobile systems and networks.

This paper aims to optimize the flight path for the UAV, energy consumption by the sensors network, the freshness of data collected from the nodes, and to minimize the error for estimating the nodes' positions when they are floating with the sea currents with assistance of only one UAV such as a fixed-wing drone.

II. RELATED WORK AND CONTRIBUTIONS

In the networks and systems mentioned above, the wireless sensor nodes were usually considered static as in [14] or with limited mobility as in [15]. It is also common to assume that these wireless nodes will periodically send their position information to a ground-based operation center and use them for data processing and to plan an optimal trajectory for the UAVs. This will not be possible if such data cannot be transmitted and there is no data link between the nodes and the operation center or between the nodes and the UAVs. It might be too complicated or expensive to secure a reliable connection between the UAVs and the wireless nodes, such as satellite communications.

These assumptions were partly relaxed in [15] by using a simple model for node motions which applies a constant ocean surface velocity at the area of interest. There are several factors considered when searching for an optimal trajectory, such as the positions, the node's energy, the priority for a specific type of sensing data, and the elapsed time since the last visit by the UAV. In addition, the UAV's flight time and the total energy consumption by the sensor nodes are also be the inputs to the optimization algorithm. It was assumed that this information is known precisely at the beginning of the mission and will be updated when the UAV gets into communication range with the nodes during the flight. For planning a new path, the last known information about the nodes will be fed to a multi-objective Particle Swarm Optimization (PSO) algorithm. PSO is a stochastic biology-inspired optimization method proposed in [16] and widely applied for instance in [17]–[19]. PSO is also used for wireless sensor networks to effectively create clusters of nodes where data collection, energy consumption and network lifetime is optimized, see [19], [20], [14].

The research in [15] showed that the position estimation error for the nodes would get significantly high (e.g., up to 10 km after a 1.5 hours flight) when the UAVs get updates from the nodes only when they are communicable of each other. Adoption of Kalman Filter (KF) improved the position estimation during the periods the UAVs could not contact the nodes. Inside this KF, a linear motion model was applied for the nodes, and the filter would estimate the node position based on any of measurements of the sea current and of the nodes position. The KF will then predict the motion until new measurement becomes available. The position errors were improved significantly (e.g., it reduces from 10 to 1 km after a 1.5 hours flight). The error increased as increasing simulation time if the KF does not get updates about ocean currents sufficiently. However, there is a challenging to secure these updates due to the locations where the sensor were deployed for example in deep ocean or the areas where it lacks of public internet connection.

Therefore, the research in this paper will one side make the assumptions more realistic, and the other side validates the system performance. Our contributions are stated as below:

1) *A realistic ocean states measurement model:* Instead of a simple model with constant ocean current as in [15], an accurate ocean model, the *Norkyst-800*, with high geographical resolution and hourly updates, will be used.

2) *Extensive simulations for practical scenarios:* Simulations and evaluations for realistic flight scenarios are the focus. Therefore, the UAV is assumed to fly periodically and each time it lasts for a limited time for example a couple of hours. The requirement that the UAV needs to fly continuously to visit the nodes is therefore removed.

3) *Kalman Filter and Particle Swarm Optimization (PSO):* The linear model of the KF will be used for predicting the positions of the nodes in the periods the UAV cannot establish communications with the nodes or during the periods there was no measurement on ocean current. PSO will be used to solve a multiple-objective optimization for producing an optimal flight path for the UAV.

III. MODELING

A. Positions prediction and state measurement models

Consider n wireless sensor nodes. Out of simplicity, we will assume that the position vector $x_i \in \mathbb{R}^2$ of node $i \in \{1, 2, \dots, n\}$ can be modeled using the difference equation $x_i(t_{k+1}) = x_i(t_k) + ha_i(t_k, x_i(t_k)) + w_i(t_k)$, with initial conditions $x_i(0) \in \mathbb{R}^2$, $h \in \mathbb{R}$ the discretization interval, $a_i(t_k, x_i(t_k)) \in \mathbb{R}^2$ is sea current velocity at the sea surface in the East-North direction, respectively, at time t_k and position x_i , and finally $w_i \sim \mathcal{N}(0, Q_i)$ is for some positive definite $Q_i \in \mathbb{R}^2$. This vector can be achieved through extracting data from *Norkyst-800* model and the process will be explained in IV-B.

A difference equation describing the motion of all the sensor nodes can therefore be given by

$$x(t_{k+1}) = x(t_k) + ha(t_k, x(t_k)) + w(t_k), \quad (1)$$

where $x = (x_1^\top, x_2^\top, \dots, x_n^\top)^\top \in \mathbb{R}^{2n}$, $a = (a_1^\top, a_2^\top, \dots, a_n^\top)^\top \in \mathbb{R}^{2n}$ (where we have left out the arguments of brevity), and $w = (w_1^\top, w_2^\top, \dots, w_n^\top)^\top \in \mathbb{R}^{2n}$.

Assuming that $\hat{a}(t, x)$ is approximation of $a(t, x)$, which is achieved from *Norkyst-800* model for instance in Norwegian coastal region. The *Norkyst-800* bathymetric grid consists of 2600×900 grid cells where each cell have an area of $800m \times 800m$. A full description is presented in [21]. The area chosen in this research is small as the movement of the nodes in the simulation period (e.g., a week or a month) is not significantly large. For more extended periods, the solution of a movable updating windows can be applied.

As the actual position x_{t_k} of the nodes at time t_k are assumed unavailable, we will use the position estimate \hat{x}_{t_k} as input to the approximation, which enable us to update the prediction of node positions in the time t_{k+1} according to:

$$\hat{x}(t_{k+1}) = \hat{x}(t_k) + h\hat{a}(t_k, \hat{x}(t_k)) \quad (2)$$

where $\hat{a}(t_k, \hat{x}(t_k)) \in \mathbb{R}^{2n}$ is the ocean surface current velocity. As explained earlier, $\hat{a}(t_k, \hat{x}(t_k))$ will be derived from the *Norkyst-800* data files at the beginning of each hour. For the period between two updates, the velocity vectors in each grid cell will remain unchanged; hence, the node position can be predicted by equation (2).

B. Node position update

We will assume that the position of a node can only be measured when the UAV is within the communication distance with the node. This was modelled in [15] as

$$y_i(t_k) = x_i(t_k) + v_i(t_k) \quad \text{if} \quad \|p(t_k) - x_i(t_k)\| \leq L_{\max} \quad (3)$$

where t_k is a specific time instance, $y_i \in \mathbb{R}^2$ is a measurement of the position of node $i \in \{1, \dots, n\}$ with some additive multivariate zero-mean normal distributed noise with covariance $R_i \in \mathbb{R}^2$, that is $v_i \sim \mathcal{N}(0, R_i)$. Furthermore, $p \in \mathbb{R}^2$ is the horizontal position of the UAV and L_{\max} is the maximal communication distance between the UAV and the nodes. A sensor normally listens to a broadcast signal from the UAV and periodically transmits its position together with sensor data only when the distance is not larger than L_{\max} . Therefore, it is reasonable to assume that the wireless sensor nodes are all equipped with a GNSS receiver, contain the same types of sensors, and will transmit the same data amount each time. Of course, it could be possible to develop a more complex configuration for the nodes, including various sensors and types.

C. Communications range for position update

The receiving radio signal strength can be described as follows.

$$Pr_{us} = Pt_0 + G_{us} - PL_{us} \quad (4)$$

where PL_{us} is propagation path loss between the UAV and a sensor node; G_{us} is the total gains of antennas on the UAV and the node; Pt_0 is transmitting power at the node. We have:

$$PL_{\max} = Pt_0 + G_{us} - Pr_{\min} \quad (5)$$

where $P_{r_{\min}}$ is the minimal power for receiving the signal. In addition, the maximal path loss PL_{\max} in the condition of Line-of-sight (LOS) is given as follows:

$$PL_{\max} = -147.55 + 20 \log f + 20 \log L_{\max} \quad (6)$$

where f [Hz] is the radio frequency, L_{\max} [m] is the maximal distance between the UAV and a sensor node. From the equations (6) and (5), L_{\max} will be determined when PL_{\max} is defined.

D. Node position estimation error

The position estimation error for a node $i \in \{1, 2, \dots, n\}$ at a sample time t_k is defined as the deviation between its referenced position $x_i(t_k) \in \mathbb{R}^2$ and the predicted position $\hat{x}_i(t_k) \in \mathbb{R}^2$. If there are N discretization points along the path of the UAV and n wireless sensor nodes, the average position estimation error in the flight period will be:

$$\bar{P} = \frac{1}{Nn} \sum_{k=1}^N \sum_{i=1}^n \|x_i(t_k) - \hat{x}_i(t_k)\| \quad (7)$$

E. Fitness function in PSO algorithm

The outputs of the PSO algorithm in this research are the optimal waypoints for the UAV to fly through and collect data from the sensor nodes so that the obtained fitness is optimal. The fitness function in this case can be defined as

$$f = \alpha_E f_E + \alpha_D f_D + \alpha_T f_T + \alpha_F f_F + \alpha_P f_P \quad (8)$$

where α_E , α_D , α_T , α_F , and α_P are positive scalar weighting constants for the functions f_E , f_D , f_T , f_F , and f_P . They stand for energy consumption by the nodes, total data collected by the UAV during a flight path, flight time for the UAV to complete the flight path, the average waiting time for the nodes to be visited by the UAV, and the nodes' position estimation error, respectively. The weight constants will be chosen to ensure a preferable order of priorities for the criterion. The larger the product of a weight constant and its respective function, the higher impact of the criteria on the final strategy of how the way-points would be selected from the PSO algorithm. For example, the priority orders are data freshness, energy consumption and flight time, then the way-points will constitute a flight path for the UAV that can visit the nodes as often as it can regardless of energy consumed by the nodes and the time for the flight. If the same data freshness was gained for different set of way-points, the PSO algorithm will start to optimize energy consumption and then flight time.

IV. SIMULATION AND RESULTS

A. Simulation Parameters

At the beginning of the mission, one can choose locations for the four sensors and then export their coordinates to a *KML* file format to retrieve velocities from *Norkyst-800* data files on *MET Norway Thredds* servers (<https://thredds.met.no/thredds/catalog/fou-hi/norkyst800m-1h/>). The output will be a subset of the *Thredds* database based on the input time range and the positions. For PSO algorithm, which optimizes the paths

TABLE I
PARAMETERS FOR PSO, UAV AND DATA TRANSMISSION

| Parameter | Value | Parameter | Value |
|----------------|--|-------------------------|--|
| n | 4 | N^{WP} | 30 |
| h_u | 120 m | v_u | 10 m/s |
| G_i | 10 dBi | G_u | 10 dBi |
| G_j | 10 dBi | $Packet$ | 800 bytes |
| $P_{r_{\min}}$ | -87 dBm | Tx_{int} | 10 s |
| P_{t_0} | 200 mW | f | 5.8 GHz |
| B | 5 MHz | $P_{r_{\min}}$ | -90 dBm |
| Lon_1 | 8.68217° | Lat_1 | 64.09803° |
| Lon_2 | 8.68206° | Lat_2 | 64.09524° |
| Lon_3 | 8.67882° | Lat_3 | 64.0966° |
| Lon_4 | 8.6855° | Lat_4 | 64.09661° |
| $Start$ | 21/7/10 00 : 00 | End | 28/7/17 00 : 00 |
| E_0 | 1000 Joule | $N^{\text{Iterations}}$ | 5000 times |
| α_E | 5 | α_D | 10 ⁷ |
| α_T | 10 ⁻² | α_F | 1 |
| α_P | 10 ² | $Noise$ | -95 dBm |
| Q_i | $\begin{bmatrix} 5 & 0 \\ 0 & 5 \end{bmatrix}$ | R_i | $\begin{bmatrix} 5 & 0 \\ 0 & 5 \end{bmatrix}$ |

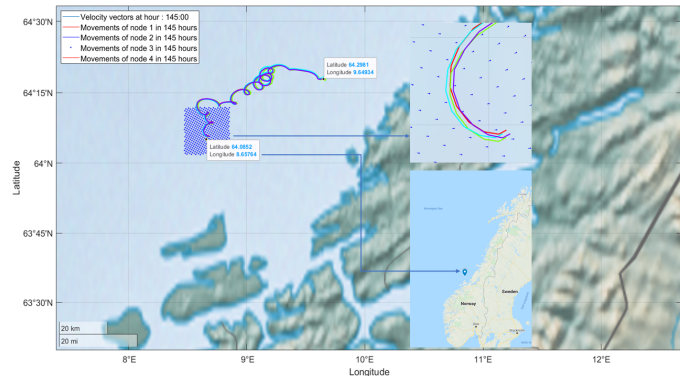


Fig. 1. Nodes motions were extracted and interpolated from *Norkyst-800*

for the UAV, we deemed that 30 waypoints (N^{WP}) would be sufficient to find a trajectory for visiting those four sensor nodes. The noise co-variances Q_i for the process model, and R_i for the measurement model are also mentioned in Table I. $Start$ and End stand for the starting, ending date and time of the simulation period.

B. Simulation Results

Based on the locations and time range defined in Table I, the velocities forecast from *Norkyst-800* and the movements of the nodes can be seen in Fig. 1. In further plotting and processing, the coordinates of the nodes and UAV were converted to local *Cartesian* coordinates North-East-Down (*NED*) with referenced *WGS-84* system. The origin of the local *NED* system with geodetic coordinates specified by Lon_i and Lat_i at ocean surface, will be chosen at the center of the initial positions of the nodes. Two scenarios explained in the following will be simulated and the results will be explained and evaluated based on factors such as position estimation error, energy consumption, obtained data rated for communications etc.

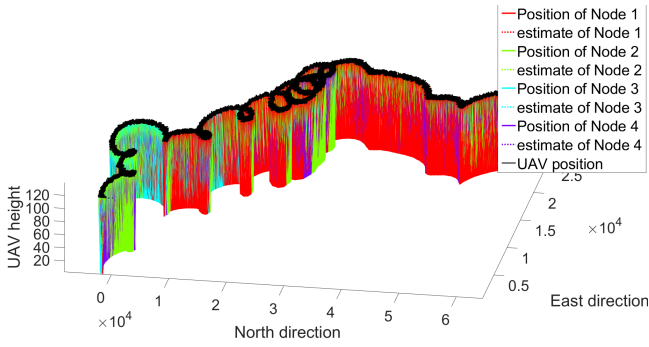


Fig. 2. Trajectories of the nodes and UAV in Scenario-1

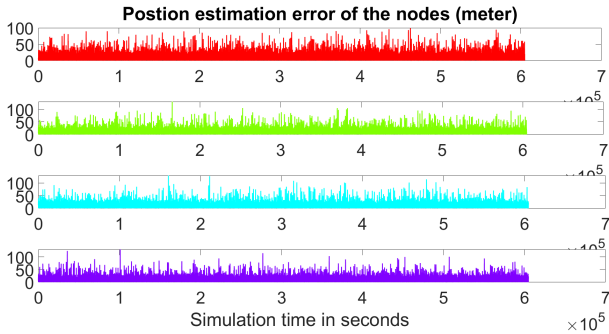


Fig. 3. Position estimation errors for the nodes in Scenario-1

1) *Scenario-1: A continuous flight:* In this situation, the UAV flies and follows the nodes' movements based on the prediction by the KF process model. The results in Fig. 2 show that in most of the simulation time, the UAV was flying over the nodes and established a constant connection with the nodes. As a result, the KF could be updated often; the position estimation error was therefore obtained at a rate of nearly *100 meters*, see Fig. 3. The data rates are also reliable at around *0.8 Mbps*, see Fig. 4. Still, the energy consumption will be an issue to the battery-powered sensor nodes as the data transmission between the nodes and the UAV is highly frequent.

2) *Scenario-2: Periodic flights:* In this scenario there are periodic flights (e.g., in every second day), and each time the UAV flies for a shorter period (e.g., can be up to few hours).

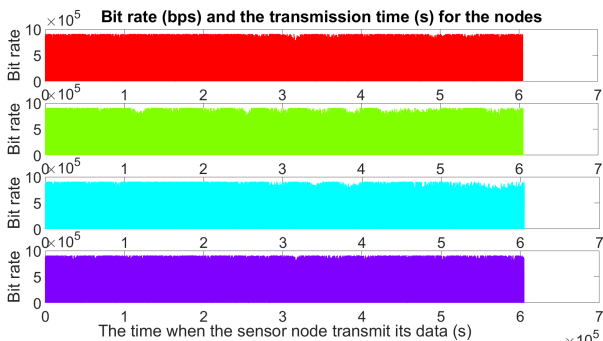


Fig. 4. Data bit rates for UAV-nodes communications in Scenario-1

With the velocities updated hourly for the KF, the achieved maximal error in positions estimation was varying between *1 and 4 km* in the entire simulation period (Figure 6). At the beginning of each flight, the nodes' position estimation error was usually high because the path planning process referred to the predicted positions for the nodes from the Kalman filter. However, this error will gradually reduce after the UAV starts its flight, due to some occasional communications with the nodes. During the idle periods between the flights, the KF will continuously predict the nodes' movements with hourly updated for the ocean velocity. Figure 5 shows the movements of the sensor nodes and the UAV during the flights in seven days. During each flight, the UAV usually gets good connection with all of the nodes and none of them was lost. The differences between the nodes' trajectories (Figures 1, 2, and 5) are relatively small because they were close to each other, at a mutual distance of around *300 meters*, at the beginning of the simulation.

The data rates for communications between the UAV and the nodes can be seen in Fig. 7. Comparing to the first scenario where the rates were almost constant at *0.8 Mbps*, the rates in the second scenario have more variations at the beginning of a flight before obtaining a more constant rate of about *0.2 Mbps* for the remaining time of the flight. A reason for this lower data rate is that the error estimation for the nodes' position was significantly high after a long idle period and the path planning for the UAV was therefore not as optimal as in the first case. Another reason is that we have prioritised the position error, flight time, and energy consumption more than the data rate in the PSO algorithm. The UAV will therefore likely receive a flight path that first leads to a minimal error in the nodes' position estimation before trying to increase the data throughput.

V. CONCLUSION

The research in this paper has addressed solutions to minimize uncertainties in predicting the movements of small floating wireless sensor nodes with the ocean stream by Kalman Filter (KF) and an assistance from the UAV. At the same time, the optimal flight path was derived from particle swarm optimization algorithm under multiple constraints. The *Norkyst-800* model was used to provide a practical estimation for the nodes' position, which are the references to the Kalman filter and to the nodes' positions prediction. The ocean velocities were assumed to be updated hourly which is the same as the model update interval, but in practice, this duration can be longer due to a lack of radio coverage, for instance when the nodes are deployed in the deep ocean or in a remote area. Based on this paper, an interesting research will be dealing with the cases the sensor nodes become more significantly separated (e.g., their mutual distances are large than the communication range). In that condition, having only one UAV will lead to a high position estimation error because of less frequent updates and some of the nodes might be lost. It will take a longer time for the UAV to fly to the predicted positions of the nodes and due to the less accuracy, the UAV

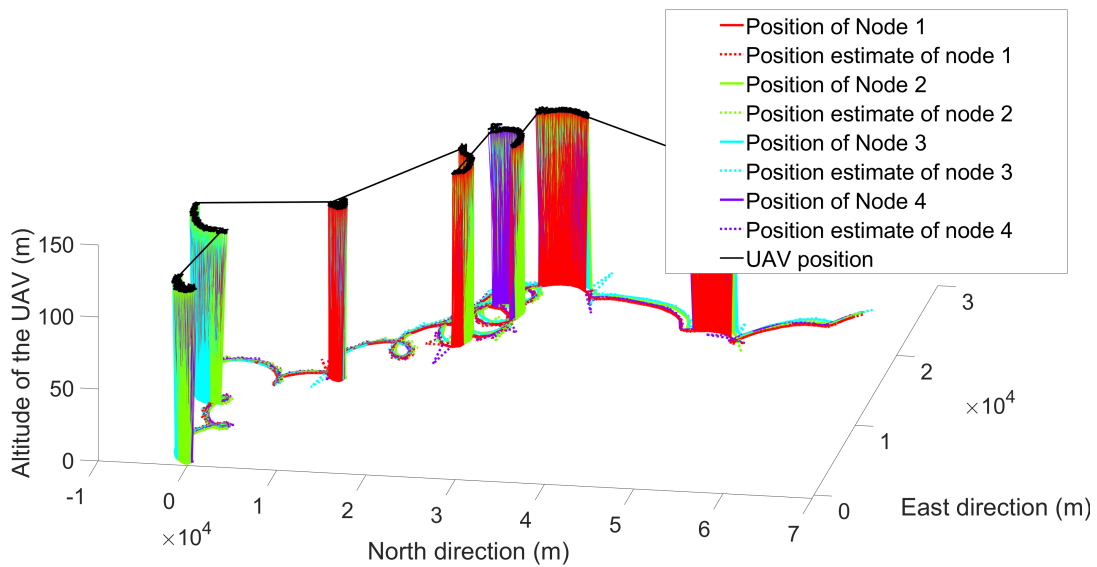


Fig. 5. Trajectories of the nodes and UAV in Scenario-2

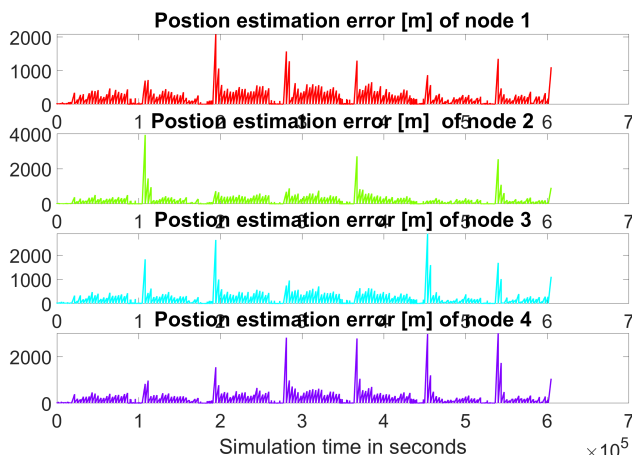


Fig. 6. Position estimation error for the nodes in Scenario-2

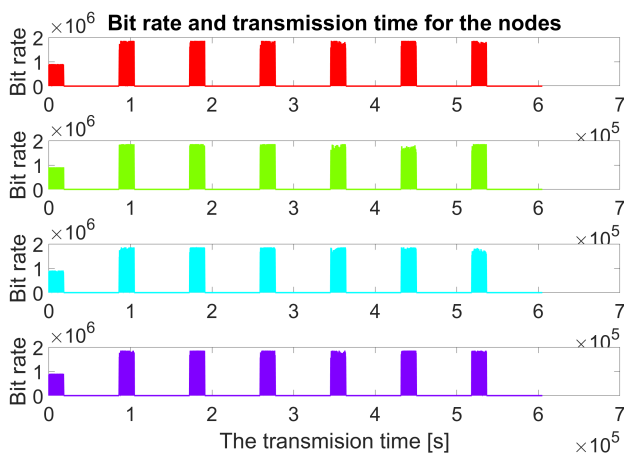


Fig. 7. Data bit rates for UAV-nodes communications in scenario-2

could be still far from the actual positions of the nodes though it follows the plan. A solution is to establish a collaborative swarm of UAVs where they could possibly maintain the mutual distance for exchanging the flight path, data collection, the nodes positions, and therefore increases the accuracy for the nodes positions estimation.

ACKNOWLEDGEMENTS

This work was partly supported by the Research Council of Norway through the Centers of Excellence funding scheme, Grant 223254.

REFERENCES

- [1] R. Ma, R. Wang, G. Liu, H.-H. Chen, and Z. Qin, "Uav-assisted data collection for ocean monitoring networks," *IEEE Network*, vol. 34, no. 6, pp. 250–258, 2020. DOI: 10.1109/MNET.011.2000168.
- [2] U. K. Verfuss, A. S. Aniceto, D. V. Harris, *et al.*, "A review of unmanned vehicles for the detection and monitoring of marine fauna," *Marine Pollution Bulletin*, vol. 140, pp. 17–29, 2019, ISSN: 0025-326X. DOI: <https://doi.org/10.1016/j.marpolbul.2019.01.009>. [Online]. Available: <https://www.sciencedirect.com/science/article/pii/S0025326X19300098>.
- [3] F. Z. Rabahi, S. Boudjit, C. Bemmoussat, and M. Benaissa, "Uavs-based mobile radars for real-time highways surveillance," in *2020 IEEE 17th International Conference on Mobile Ad Hoc and Sensor Systems (MASS)*, 2020, pp. 80–87. DOI: 10.1109/MASS50613.2020.00020.

- [4] R. Madhavan, T. Silva, F. Farina, R. Wiebbelling, L. Renner, and E. Prestes, "Unmanned aerial vehicles for environmental monitoring, ecological conservation, and disaster management," in *Technologies for Development*, Springer, 2018, pp. 31–39, ISBN: 978-3-319-91068-0.
- [5] T. Noguchi and Y. Komiya, "Persistent cooperative monitoring system of disaster areas using uav networks," in *2019 IEEE SmartWorld, Ubiquitous Intelligence Computing, Advanced Trusted Computing, Scalable Computing Communications, Cloud Big Data Computing, Internet of People and Smart City Innovation (SmartWorld/SCALCOM/UIC/ATC/CBDCom/IOP/SCI)*, 2019, pp. 1595–1600. DOI: 10.1109/SmartWorld-UIC-ATC-SCALCOM-IOP-SCI.2019.00285.
- [6] P. -. Radoglou, P. Sarigiannidisa, T. Lagkasbc, and M. Ioannis, "A compilation of UAV applications for precision agriculture," *Computer Networks*, vol. 172, no. 107148, May 2020.
- [7] C. Kyrkou and T. Theocharides, "Deep-learning-based aerial image classification for emergency response applications using unmanned aerial vehicles," in *2019 IEEE/CVF Conference on Computer Vision and Pattern Recognition Workshops (CVPRW)*, 2019, pp. 517–525. DOI: 10.1109/CVPRW.2019.00077.
- [8] S. K. Khan, U. Naseem, A. Sattar, *et al.*, "Uav-aided 5g network in suburban, urban, dense urban, and high-rise urban environments," in *2020 IEEE 19th International Symposium on Network Computing and Applications (NCA)*, 2020, pp. 1–4. DOI: 10.1109/NCA51143.2020.9306710.
- [9] Y. Gao, J. Cao, P. Wang, *et al.*, "Uav based 5g wireless networks: A practical solution for emergency communications," in *2020 XXXIIIrd General Assembly and Scientific Symposium of the International Union of Radio Science*, 2020, pp. 1–4. DOI: 10.23919/URSIGASS49373.2020.9232188.
- [10] J. Zhang, F. Liang, B. Li, Z. Yang, Y. Wu, and H. Zhu, "Placement optimization of caching uav-assisted mobile relay maritime communication," *China Communications*, vol. 17, no. 8, pp. 209–219, 2020. DOI: 10.23919/JCC.2020.08.017.
- [11] T. A. Johansen, A. Zolich, T. Hansen, and A. J. Sørensen, "Unmanned aerial vehicle as communication relay for autonomous underwater vehicle - field tests," in *IEEE Globecom Workshop - Wireless Networking and Control for Unmanned Autonomous Vehicles*, Austin, TX, 2014.
- [12] A. Zolich, T. A. Johansen, A. Sægrov, E. Vågsholm, and V. Hovstein, "Coordinated maritime missions of unmanned vehicles - network architecture and performance analysis," in *IEEE ICC 2017 Mobile and Wireless Networking*, Paris, 2017.
- [13] B. Li, Z. Fei, and Y. Zhang, "Uav communications for 5g and beyond: Recent advances and future trends," *IEEE Internet of Things Journal*, vol. 6, no. 2, pp. 2241–2263, 2019.
- [14] T. D. Ho, E. I. Grøtli, P. B. Sujit, T. A. Johansen, and J. B. Sousa, "Optimization of wireless sensor network and uav data acquisition," *Journal of Intelligent and Robotic Systems*, vol. 78, pp. 159–179, Mar. 2015.
- [15] T. Dac Ho, E. Ingar Grøtli, and T. Arne Johansen, "Pso and kalman filter-based node motion prediction for data collection from ocean wireless sensors network with uav," in *2021 IEEE International Conference on Consumer Electronics (ICCE)*, 2021, pp. 1–7. DOI: 10.1109/ICCE50685.2021.9427697.
- [16] J. Kennedy and R. Eberhart, "Particle swarm optimization," in *Proceedings of ICNN'95 - International Conference on Neural Networks*, vol. 4, 1995, 1942–1948 vol.4.
- [17] W. Li, "PSO based wireless sensor networks coverage optimization on dems," in *Advanced Intelligent Computing Theories and Applications. With Aspects of Artificial Intelligence*, Springer, 2012, pp. 371–378, ISBN: 978-3-642-25944-9.
- [18] Y. Yang, B. Li, and B. Ye, "Wireless sensor network localization based on pso algorithm in nlos environment," in *2016 8th International Conference on Intelligent Human-Machine Systems and Cybernetics (IHMSC)*, vol. 01, 2016, pp. 292–295.
- [19] S. Jiang, "Leach protocol analysis and optimization of wireless sensor networks based on pso and ac," in *2018 10th International Conference on Intelligent Human-Machine Systems and Cybernetics (IHMSC)*, vol. 02, 2018, pp. 246–250.
- [20] C. Huang and J. Fei, "Uav path planning based on particle swarm optimization with global best path competition," *International Journal of Pattern Recognition and Artificial Intelligence*, vol. 32, Oct. 2017. DOI: 10.1142/S0218001418590085.
- [21] A. Jon, S. A. Kristin, S. André, S. A. Dagrund, V. Frode, and A. Lars, "Norkyst-800 report no. 1: User manual and technical descriptions," Institute of Marine Research, Tech. Rep. 2/2011, Feb. 2011, p. 43. [Online]. Available: <http://hdl.handle.net/11250/113865>.